Fast and Accurate Quantum Molecular Dynamics of Dense Plasmas Across Temperature Regimes

Travis Sjostrom and Jérôme Daligault
Theoretical Division, Los Alamos National Laboratory, Los Alamos, New Mexico 87545, USA
(Received 25 July 2014; published 10 October 2014)

We develop and implement a new quantum molecular dynamics approximation that allows fast and accurate simulations of dense plasmas from cold to hot conditions. The method is based on a carefully designed orbital-free implementation of density functional theory. The results for hydrogen and aluminum are in very good agreement with Kohn-Sham (orbital-based) density functional theory and path integral Monte Carlo calculations for microscopic features such as the electron density as well as the equation of state. The present approach does not scale with temperature and hence extends to higher temperatures than is accessible in the Kohn-Sham method and lower temperatures than is accessible by path integral Monte Carlo calculations, while being significantly less computationally expensive than either of those two methods.

DOI: 10.1103/PhysRevLett.113.155006 PACS numbers: 52.65.-y, 52.25.Kn, 71.15.Mb, 71.15.Pd

A significant challenge of high energy density physics is the determination of the fundamental properties of plasmas (e.g., equation of state, transport properties) over a wide range of temperatures and densities [1,2]. Systems of particular focus include warm dense matter [3], inertial confinement fusion, notably, the compression pathway to ignition, and astrophysical plasmas. Two methods have emerged as standards for such calculations which have yielded quality results. Those are quantum molecular dynamics based on the Kohn-Sham density functional theory (DFT) [4–6] and path integral Monte Carlo (PIMC) calculations [7,8]. Because of the nature of the method, PIMC calculations become prohibitive as the temperature is decreased and Kohn-Sham DFT becomes prohibitive with increasing temperature as the number of required orbitals increases with temperature and, in general, the method scales as the cube of the number of orbitals. It is possible to find the region of overlap for these calculations, but such a region is generally difficult for both methods [8,9]. For example, with deuterium at 4 g/cc overlap, calculations have be done at temperatures 5–20 eV, while for carbon very expensive overlap calculations have been done from 40 to 60 eV; for still heavier elements such as aluminum and iron, PIMC calculations do not exist and Kohn-Sham molecular dynamics have not been pushed much above 10 eV [10,11]. In this Letter, we develop and implement an orbital-free DFT formulation which provides accuracy at the level of Kohn-Sham DFT and PIMC calculations at significantly lower cost, while spanning from low to high temperatures.

In DFT, the fundamental quantity is the free energy, which is minimized to find the electron density. For a given ionic configuration the free energy is a functional of the electron density n and is given by [12]

$$F[n] = F_s[n] + F_H[n] + F_{xc}[n] + F_{ei}[n], \qquad (1)$$

where F_s is the noninteracting free energy comprised of both kinetic and entropic parts, F_H is the Hartree energy or direct Coulomb interaction between the electrons, F_{ei} is the electron-ion Coulomb interaction, and F_{xc} is defined as the remainder of the total free energy, which includes the quantum mechanical exchange and correlation as well as the excess kinetic and entropic terms. Of the contributions, neither F_s nor F_{xc} have explicitly calculable forms. Given the same orbital-free F_{xc} approximation, the only difference in the approach of the orbital-free DFT from the Kohn-Sham DFT is that the noninteracting free energy F_s is approximated by a density functional instead of being exactly obtained through the calculation of single particle orbitals [13]. Thus, the orbital-free DFT [3] returns to a pure DFT which, as given by the Hohenberg-Kohn-Mermin theorems [14,15], is an exact theory.

Significant efforts have been made at zero temperature in developing advanced orbital-free functionals with high quality results [16–22]. Though without analogous efforts, in recent years the orbital-free approach at finite temperature has gained attention, with most results being for hot dense systems where the venerable Thomas-Fermi approximation is employed for F_s [23–25]. The work of Perrot offered a density gradient correction to Thomas-Fermi that improves results moderately [26,27]. Other more recent semilocal functionals [28] have also been considered. None of these functionals, though, have reached the accuracy of Kohn-Sham across temperature regimes.

In this work we develop and implement an advanced density functional for F_s, valid at zero temperature as well as finite temperature, which provides a highly accurate agreement with the Kohn-Sham results, yet is temperature independent in computational cost, since the dependence is on the density only.

We now give a summary of our functional. Further details of individual terms, and all other quantities necessary for quantum molecular dynamics implementation are given in the Supplemental Material [29]. The proposed functional for the noninteracting free energy is of the following form:

$$F_s[n] = F_{TF}[n] + {}_{\beta}F_{vW}[n] + F_{a,b}[n]. \tag{2}$$

Here the first term on the rhs is the familiar Thomas-Fermi [30] term

$$F_{TF}[n] = \int f_{TF}(n(\mathbf{r}))d\mathbf{r}, \tag{3}$$

where f_{TF} is just the noninteracting electron gas energy per volume at density n. The second term on the rhs is the proposed extension of the semilocal von Weiszäcker term

$$\begin{aligned} {}_{\beta}F_{vW}[n] = \frac{\hbar^2}{2m_e}\iint &[(\nabla n^{1/2}(\mathbf{r}))\cdot(\nabla n^{1/2}(\mathbf{r}'))] \\ &\times[\delta(\mathbf{r}-\mathbf{r}') + \beta(|\mathbf{r}-\mathbf{r}'|)]d\mathbf{r}'d\mathbf{r}. \end{aligned} \tag{4}$$

In the limit $\beta(|\mathbf{r}-\mathbf{r}'|) = 0$ this reduces to the standard von Weiszäcker [31] term

$$F_{vW}[n] = \frac{\hbar^2}{m_e}\int \frac{|\nabla n(\mathbf{r})|^2}{8n(\mathbf{r})}d\mathbf{r}. \tag{5}$$

The final term is a nonlocal density contribution to the free energy [32]

$$F_{a,b}[n] = \iint n^a(\mathbf{r})w(|\mathbf{r}-\mathbf{r}'|)n^b(\mathbf{r}')d\mathbf{r}'d\mathbf{r}. \tag{6}$$

with a and b free parameters, and chosen to be $a = b = 5/6$.

This leaves still undetermined the kernels β and w. To proceed, the functional is constrained to reproduce the exact density-density response function (Lindhard), $\tilde{\chi}_0$, of the noninteracting uniform electron gas as follows:

$$\tilde{\chi}_0^{-1}(k; n_0, T) = -\hat{\mathrm{F}}\left(\frac{\delta^2 F_S[n,T]}{\delta n(\mathbf{r})\delta n(\mathbf{r}')}\bigg|_{n_0}\right). \tag{7}$$

Here $\hat{\mathrm{F}}$ denotes the Fourier transform of the second functional derivative of F_s evaluated at the average density n_0. This results in the following relation for the w and β kernels in reciprocal space:

$$\begin{aligned} \tilde{w}(k) &= \frac{-\tilde{\chi}_0^{-1}(k) + \tilde{\chi}_{TF}^{-1} + [1+\tilde{\beta}(k)]\tilde{\chi}_{vW}^{-1}(k)}{2abn_0^{(a+b-2)}} \\ &\equiv f(k)\frac{-\tilde{\chi}_0^{-1}(k) + \tilde{\chi}_{TF}^{-1} + \tilde{\chi}_{vW}^{-1}(k)}{2abn_0^{(a+b-2)}}, \end{aligned} \tag{8}$$

where $\tilde{\chi}_{TF}^{-1}$ and $\tilde{\chi}_{vW}^{-1}(k)$ are the contributions to Eq. (7) from Eq. (3) and Eq. (5), respectively. For convenience we have written $\tilde{w}$ in terms of $f(k)$ in the second line. We may now choose $f(k)$ with the only constraint that $f(k)$ remains finite. The satisfaction of Eq. (8) then determines $\tilde{w}$ and $\tilde{\beta}$, and guarantees the functional produces the exact response and free energy in the uniform electron gas limit.

At zero temperature [16–20] and more recently at finite temperature [32], the case $f \equiv 1$ (i.e., $\beta \equiv 0$), has been investigated. Though this case meets the requirement of correcting the response, it produces a kernel $\tilde{w}$ which goes to the constant negative value in the large k limit ($k > 10k_F$) and thus results in the functional being unbounded and producing unphysical densities with infinitely negative energy [33]. We have added the nonlocality β in Eq. (4) to alleviate this issue, while still enforcing the exact response. In order to force $\tilde{w}(k)$ to zero for large k ($k > 10k_F$), removing the aforementioned difficulty of the $f \equiv 1$ case, we consider the interpolating $f(k) = e^{-k^2/\alpha^2 k_F^2}$ with $\alpha = 4$.

We have applied the new functional to hydrogen and aluminum over a wide range of density and temperatures. In these calculations we use a local pseudopotential for all orbital-free calculations as well as for some Kohn-Sham calculations. Using the same pseudopotential provides an apple to apple comparison of our F_s functional to the exact Kohn-Sham method for F_s, since we also use the same F_{xc} approximation in all cases. In addition, we perform Kohn-Sham calculations with a more standard nonlocal pseudopotential for comparison.

The details of the calculations are as follows. The local pseudopotentials for hydrogen and aluminum are given in Refs. [28] and [34], respectively. In the orbital-free calculations the numeric grid sizes were 64^3 or 96^3 depending on system size and density. For the Kohn-Sham calculations we used the QUANTUM-ESPRESSO code [35] and plane wave cutoff energies of 2040 and 680 eV for hydrogen and aluminum, respectively, and all calculations were done at the Gamma point only. All calculations use the local density approximation [36] for F_{xc}.

First we consider the computational cost. The time required for the optimization of the electron density for a given random arrangement of 128 hydrogen atoms at density 2 g/cm^3 at various temperatures is shown in Fig. 1, as calculated on an eight-core 2.93 GHz Intel Xeon machine. This corresponds to the time for a single molecular dynamics time step. For the Kohn-Sham case, the temperature scaling is clearly shown as a bottleneck to higher temperature simulations as the time goes from under

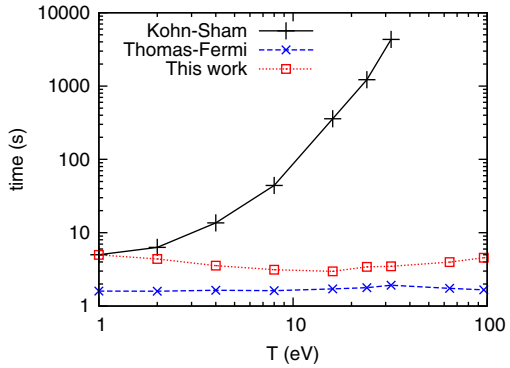

FIG. 1 (color online). Time for a single electron density optimization for 128 hydrogen atoms in a given random arrangement at 2 g/cm^3. The Kohn-Sham temperature scaling is clearly shown as a prohibitive factor in extending across temperature regimes, while our functional shows no such issue.

10 s at 1 eV to over 1200 s at 24 eV and over 4300 s at 32 eV. The required number of orbitals goes from 100 to 1600 to 2400, respectively, to achieve a threshold occupation of 10^{-6}. In contrast for the orbital-free methods there is no scaling with temperature. Our functional took generally 4–6 s whereas the simpler Thomas-Fermi calculations took about 2 s. It is of note that though the nonlocal terms of Eqs. (4) and (6) appear computationally expensive, they may be evaluated efficiently in reciprocal space through the use of fast Fourier transforms.

Next we consider an important microscopic feature, the electron density, which by the primary tenet of DFT determines the system completely. Other integrated quantities, such as the total energy or pressure, which are often alone considered in determining the accuracy of a functional, are important results. However, if one achieves good results in those integrated quantities and not in the density itself, the integrated results are good due to some cancellation of errors. So we begin with the electron density examined through the ion-electron pair distribution function, g_{ie}. Recall that $n(r) = n_0 g_{ie}(r)$ is the average electron density around an ion. In Fig. 2 the results of three orbital-free functionals are plotted. These include the Thomas-Fermi approximation, as well as the Perrot functional, and our new functional given in this work. As explained before the only difference between these orbital-free calculations and the Kohn-Sham local pseudopotential (LPP) calculation is in F_s. The most remarkable feature is that the Kohn-Sham (LPP) and our functional produce nearly identical g_{ie} or electron densities. On the contrary, the simpler functionals produce quite different densities. We also solve the Kohn-Sham system with the more standard approach of a nonlocal pseudopotential (NLPP). Comparing the Kohn-Sham (NLPP) results we see good agreement for the hydrogen case over the whole range and good agreement for aluminum outside the pseudopotential cutoff radius, around $r/r_{\mathrm{ws}} = 0.6$.

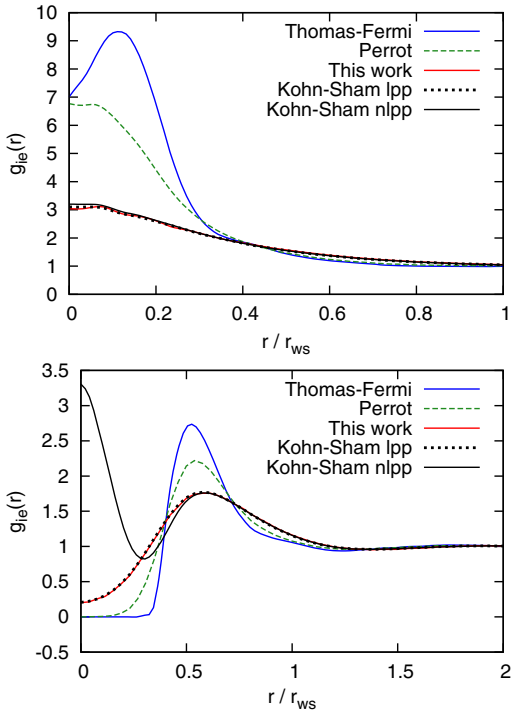

FIG. 2 (color online). Top: The ion-electron pair correlation function $g_{ie}(r)$ is plotted for a random distribution of hydrogen atoms at density 2 g/cc and temperature of 5 eV. Bottom: The same but for aluminum at 2.8 g/cc and temperature 100 K = 0.008 617 eV. r_{ws} is the ion Wigner-Seitz radius. Both systems show excellent agreement for the electron densities between our functional and Kohn-Sham, where the same pseudopotential is used.

Next we consider two cases of fixed ions. First, we consider hydrogen as a simple-cubic lattice at 2 g/cc and temperatures from 1 to 1000 eV. In the top panel of Fig. 3 the pressure is plotted up to 10 eV for the functionals and pseudopotentials as previously described. Here at fixed density the increase in pressure with temperature is completely due to the thermal excitation of the electrons. The maximum difference between the Kohn-Sham (NLPP) results and our functional is less than 0.5%, whereas the maximum difference for the Thomas-Fermi and Perrot functionals are 24% and 14%, respectively. Above 40 eV the differences between the functionals is negligible. In the lower panel we consider face-center-cubic aluminum at 100 K = 0.008 617 eV near equilibrium density. Here again there is excellent agreement for the present functional and Kohn-Sham methods. The simple Thomas-Fermi functional does not exhibit any binding, as indicated by the pressure becoming negative, and while the Perrot correction does it is significantly different from the results of Kohn-Sham and our functional.

Now we consider molecular dynamics simulations for warm dense deuterium and aluminum. Note, deuterium is examined to connect with the PIMC data, and involves the same pseudopotentials as for hydrogen. Equation of state

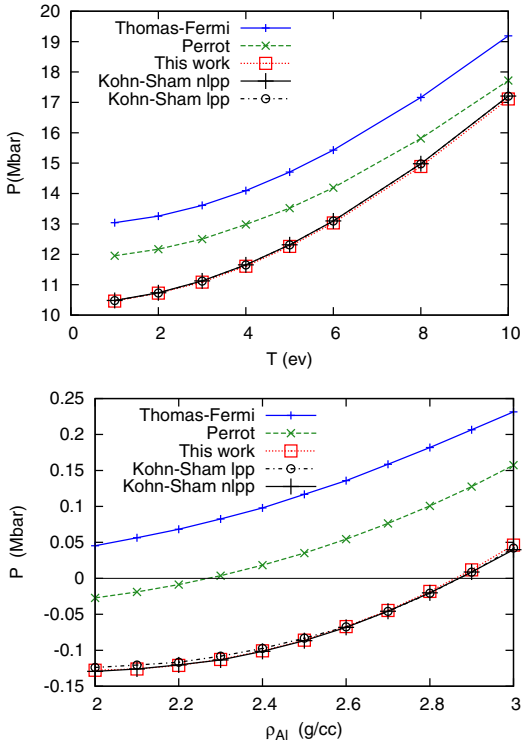

FIG. 3 (color online). Pressure results for simple-cubic hydrogen at 2 g/cc (top) and for fcc aluminum at 100 K = 0.008 617 eV (bottom). Both results show our functional closely reproducing Kohn-Sham results.

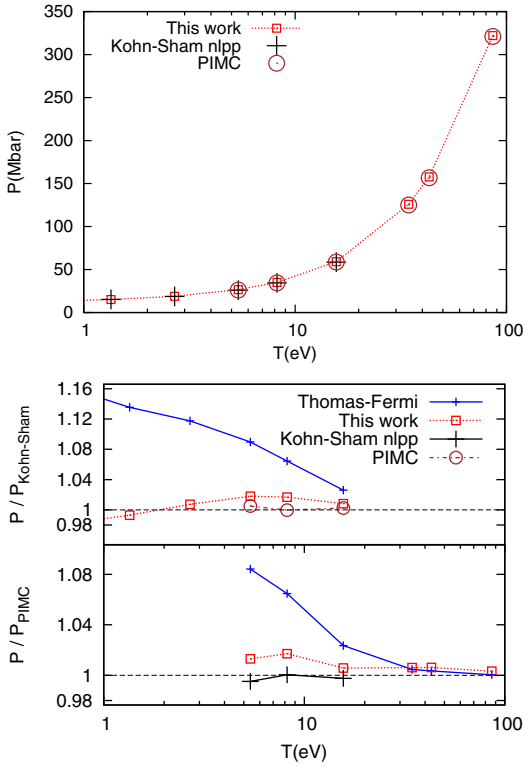

FIG. 4 (color online). Pressure results for deuterium at 4.048 19 g/cc. Our functional is in good agreement with Kohn-Sham and PIMC calculations and spans the entire temperature range. The bottom panel shows the relative pressure with Kohn-Sham and PIMC calculations in their respective ranges.

results are plotted for deuterium at 4.048 19 g/cc and temperatures from 1 to 100 eV in Fig. 4. In addition, Kohn-Sham results are plotted up to 15.7 eV and path integral Monte Carlo [7] results down to 5.4 eV. While the Kohn-Sham method becomes computationally prohibitive with increasing temperature, the PIMC does so with decreasing temperature. The present orbital-free calculations, however, span the entire temperature range and are significantly less expensive than the other methods at any temperature while showing good agreement with both the Kohn-Sham and PIMC calculations in their respective regions of applicability. Specifically our functional results never deviate by more than 2% from either the Kohn-Sham or PIMC results. Similar results have been obtained at 1.0 and 10.0 g/cc as well (not shown). We note also that for dilute systems, such as deuterium below 0.5 g/cc, accuracy does diminish. For both the orbital-free and Kohn-Sham calculations 128 atoms were simulated for 10 000 and 5000 time steps, respectively. The times steps varied with temperature from 0.5 fs at 1 eV to 0.0125 fs at 100 eV. At 15.7 eV the Kohn-Sham calculation took 161.5 s per time step on 48 compute cores, while the orbital-free calculation took 1.76 s per time step on 32 compute cores on the same machine.

For the case of aluminum we have calculated the ion-ion pair distribution function g_{ii} for two cases. The first is near melting at the experimental density and the temperature of 2.349 g/cc and 1023 K = 0.088 15 eV. The second is the warm dense case of 2.7 g/cc and 5 eV. Figure 5 shows g_{ii} for both cases. Our functional and the Kohn-Sham results are in very good agreement in both cases and the experimental data [37] are also in agreement at the lower temperature. Here, g_{ii} was averaged over 15 000 and 6000 time steps for 108 and 64 atoms after equilibration in the orbital-free and Kohn-Sham calculations, respectively.

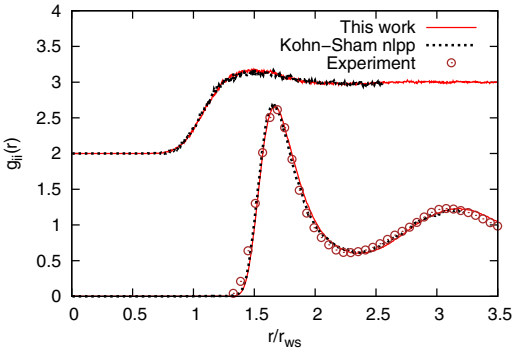

FIG. 5 (color online). Pair distribution function $g_{ii}(r)$ for Al at experimental density 2.349 g/cc and temperature 1023 K = 0.088 15 eV (lower curves) and warm dense conditions 2.7 g/cc and 5 eV (upper curves, shifted by 2). Excellent agreement is shown between the Kohn-Sham and our functional.

In summary, the present orbital-free functional shows excellent agreement with the Kohn-Sham results while being computationally less expensive and having applicability to regions of higher temperature than are accessible by Kohn-Sham methods, as well as very good agreement with PIMC calculations at high temperatures while reaching lower temperatures than those accessible by PIMC calculations. The strong agreement in the $g_{ie}(r)$, as compared with the Kohn-Sham method, shows also that the current results are truly reproducing orbital-based results and as such demonstrate a realization of a highly accurate pure density functional theory. In future work we will consider more complex systems with higher atomic number elements as well as mixtures and lower density systems such as expanded metals.

This work was carried out under the auspices of the National Nuclear Security Administration of the U.S. Department of Energy (DOE) at Los Alamos National Laboratory under Contract No. DE-AC52-06NA25396. The work was supported by the DOE Office of Fusion Sciences.

[1] R. P. Drake, Phys. Today **63**, No. 6, 28 (2010).
[2] U.S. Department of Energy, Office of Science and National Nuclear Security Administration, Basic Research Needs for High Energy Density Laboratory Physics, Report of the Workshop on High Energy Density Laboratory Physics Research Needs, November 15–18, 2009 (2010).
[3] *Frontiers and Challenges in Warm Dense Matter*, edited by F. Graziani, M. P. Desjarlais, R. Redmer, and S. B. Trickey, Lecture Notes in Computational Science and Engineering, Vol. 96 (Springer, New York, 2014).
[4] S. Mazevet, F. Lambert, F. Bottin, G. Zèrah, and J. Clèrouin, Phys. Rev. E **75**, 056404 (2007).
[5] B. Holst, R. Redmer, and M. P. Desjarlais, Phys. Rev. B **77**, 184201 (2008).
[6] C. Wang and P. Zhang, Phys. Plasmas **20**, 092703 (2013).
[7] S. X. Hu, B. Militzer, V. N. Goncharov, and S. Skupsky, Phys. Rev. B **84**, 224109 (2011).
[8] K. P. Driver and B. Militzer, Phys. Rev. Lett. **108**, 115502 (2012).
[9] B. Militzer, Phys. Rev. B **79**, 155105 (2009).
[10] L. X. Benedict, K. P. Driver, S. Hamel, B. Militzer, T. Qi, A. A. Correa, A. Saul, and E. Schwegler, Phys. Rev. B **89**, 224109 (2014).
[11] C. Wang, Z.-B. Wang, Q.-F. Chen, and P. Zhang, Phys. Rev. E **89**, 023101 (2014).
[12] R. G. Parr and W. Yang, *Density-Functional Theory of Atoms and Molecules* (Oxford, New York, 1989).
[13] W. Kohn and L. J. Sham, Phys. Rev. **140**, A1133 (1965).
[14] P. Hohenberg and W. Kohn, Phys. Rev. **136**, B864 (1964).
[15] N. David Mermin, Phys. Rev. **137**, A1441 (1965).
[16] L.-W. Wang and M. P. Teter, Phys. Rev. B **45**, 13196 (1992).
[17] E. Smargiassi and P. A. Madden, Phys. Rev. B **49**, 5220 (1994).
[18] F. Perrot, J. Phys. Condens. Matter **6**, 431 (1994).
[19] Y. A. Wang, N. Govind, and E. A. Carter, Phys. Rev. B **58**, 13465 (1998).
[20] Y. A. Wang, N. Govind, and E. A. Carter, Phys. Rev. B **60**, 16350 (1999).
[21] G. S. Ho, V. L. Lignères, and E. A. Carter, Comput. Phys. Commun. **179**, 839 (2008).
[22] D. J. Gonzalez, L. E. Gonzalez, J. M. Lopez, and M. J. Stott, Phys. Rev. B **65**, 184201 (2002).
[23] F. Lambert, J. Clèrouin, and G. Zèrah, Phys. Rev. E **73**, 016403 (2006).
[24] L. Burakovsky, C. Ticknor, J. D. Kress, L. A. Collins, and F. Lambert, Phys. Rev. E **87**, 023104 (2013).
[25] J. Clèrouin, G. Robert, P. Arnault, J. D. Kress, and L. A. Collins, Phys. Rev. E **87**, 061101(R) (2013).
[26] F. Perrot, Phys. Rev. A **20**, 586 (1979).
[27] J.-F. Danel, L. Kazandjian, and G. Zèrah, Phys. Plasmas **15**, 072704 (2008).
[28] V. V. Karasiev, T. Sjostrom, and S. B. Trickey, Phys. Rev. B **86**, 115101 (2012).
[29] See Supplemental Material at http://link.aps.org/supplemental/10.1103/PhysRevLett.113.155006 for orbital-free functional implementation details.
[30] R. P. Feynman, N. Metropolis, and E. Teller, Phys. Rev. **75**, 1561 (1949).
[31] C. F. von Weizsäcker, Z. Phys. **96**, 431 (1935).
[32] T. Sjostrom and J. Daligault, Phys. Rev. B **88**, 195103 (2013).
[33] X. Blanc and E. Cancès, J. Chem. Phys. **122**, 214106 (2005).
[34] C. Huang and E. A. Carter, Phys. Chem. Chem. Phys. **10**, 7109 (2008).
[35] P. Giannozzi *et al.*, J. Phys. Condens. Matter **21**, 395502 (2009).
[36] J. P. Perdew and A. Zunger, Phys. Rev. B **23**, 5048 (1981).
[37] Structural Characterization of Materials Liquid Database, Institute of Advanced Materials Processing, Tohoku University, Japan, 1979, http://res.tagen.tohoku.ac.jp/~waseda/scm/index.html.